

Received: March 12, 1986; accepted: May 20, 1986

PREPARATION AND CHARACTERIZATION OF Ni(SbF₆)₂

KARL O. CHRIS^{*}TE, WILLIAM W. WILSON
Rocketdyne, A Division of Rockwell International
Canoga Park, California 91303 (USA)

ROLAND A. BOUGON and PIERRETTE CHARPIN
Centre d'Etudes Nucléaires de Saclay,
91191 Gif sur Yvette, Cédex (France)

SUMMARY

Ni(SbF₆)₂ was prepared from Ni powder, F₂ and SbF₅ at 270°C and 250 atm pressure. The yellow, crystalline material is stable to at least 230°C and was characterized by elemental analysis, x-ray powder data, and vibrational spectroscopy. The crystal structure of Ni(SbF₆)₂, (hexagonal, a = 5.16Å, c = 27.90Å, Z = 3), can be related to the rhombohedral-hexagonal LiSbF₆ structure by occupation of only every second Li⁺ site with Ni²⁺ and by the concomitant doubling of the c-axis of its hexagonal unit cell.

INTRODUCTION

In high temperature fluorination reactions involving elemental fluorine and a strong Lewis acid in a metal cylinder, the metal cylinder is usually strongly attacked by the reagents. To minimize these side reactions, cylinders made from either nickel or nickel-copper alloys, such as Monel, are generally used. Even under these conditions the attack on the cylinder is still appreciable and often can compete with the desired reactions [1-3]. Although it has repeatedly been stated that the side products in F₂-MF₅ (M=As,Sb,Bi) reactions in nickel reactors are Ni(MF₆)₂ salts [1-3], very few data have been

published for these compounds. For $\text{Ni}(\text{AsF}_6)_2$, only its x-ray powder pattern and vibrational spectra [4] and, for $\text{Ni}(\text{SbF}_6)_2$, only its magnetic moment [5] have been published. In view of the fact that these salts are very common impurities in most high-temperature, high-pressure fluorination reactions involving these Lewis acids and fluorine, a better characterization of these nickel salts was highly desirable.

EXPERIMENTAL

Apparatus

Fluorine (Air Products) was handled in a conventional stainless steel-Teflon FEP vacuum line. Solids and SbF_5 (Ozark Mahoning, purified by vacuum distillation prior to use) were handled in the dry nitrogen atmosphere of a glove box. Infrared spectra were recorded on a Perkin Elmer Model 283 spectrometer. Raman spectra were recorded on a Spex Model 1403 spectrophotometer using the 647.1 nm exciting line of a Kr-ion laser and melting point capillaries as sample containers. X-ray diffraction patterns were obtained using 0.5 mm quartz capillaries, a General Electric Model XRD-6 diffractometer, Ni-filtered CuK_α radiation, and a 114.6 mm diameter Phillips camera.

$\text{Ni}(\text{SbF}_6)_2$

Nickel powder (7.968 mmol) was placed into a 20 mL nickel cylinder equipped with a nickel valve. The cylinder containing the Ni powder was passivated at ambient temperature with 2 atm of gaseous F_2 for 2.5 hr. The F_2 was pumped off and distilled SbF_5 (53.80 mmol) was added to the cylinder in the dry box. The cylinder was connected to a stainless steel vacuum line, evacuated and cooled to -196°C . Fluorine (60.5 mmol) was condensed into the cylinder, and the cylinder was allowed to warm to ambient temperature behind a barricade. The cylinder was placed into an oven and heated

to 270°C for 88 hr, cooled, and then reconnected to the vacuum line. The excess of F₂ was pumped off at room temperature, and the reactor was heated in a dynamic vacuum to 180°C for 7 hr. The yellow crystalline residue (14.257g, weight calcd. for 26.90 mmol of Ni(SbF₆)₂ = 14.262g) did not lose any weight on heating to 230°C for 4 hr in a dynamic vacuum. Anal. Calcd for Ni(SbF₆)₂: Ni, 11.07; Sb, 45.93; F, 43.00. Found: Ni, 11.22; Sb, 46.20; F, 42.67.

RESULTS AND DISCUSSION

Synthesis and Properties of Ni(SbF₆)₂

The reaction of F₂ and SbF₅ with nickel powder was carried out in a nickel reactor at 270°C and about 250 atm pressure. It resulted not only in a quantitative conversion of the nickel powder to Ni(SbF₆)₂, but also in an attack on the walls of the nickel vessel until the limiting reagent, SbF₅, was completely consumed by formation of Ni(SbF₆)₂. The product was a finely divided, pale yellow, hygroscopic, crystalline powder which is stable in a dynamic vacuum up to at least 230°C. Its composition was established by the observed material balance and elemental analysis. It readily dissolves in water with the green color characteristic for aqueous solutions of Ni²⁺. With CH₃CN it forms a bright blue solid and solution. By analogy with the known [6] compound [Ni(CH₃CN)₆]²⁺(BF₄⁻)₂, the blue color suggests the formation of the corresponding [Ni(CH₃CN)₆]²⁺(SbF₆⁻)₂ complex. In anhydrous HF, Ni(SbF₆)₂ is quite soluble. Large cube-shaped crystals were grown from this solvent. However, they tended to be multiple crystals, thus preempting a crystal structure determination.

X-Ray Diffraction Data

Due to the lack of suitable single crystals, only powder data could be recorded for Ni(SbF₆)₂. The observed pattern (see Table I)

closely resembles those previously reported for the hexagonal-rhombohedral AMF_6 -type compounds $LiBiF_6$ and $NaBiF_6$ [7]. These compounds are isotypic with $LiSbF_6$ whose structure is well known from single crystal data and can be considered as a rhombohedrally distorted, face-centered cubic $NaSbF_6$ -type structure [8].

Replacement of the singly charged Li^+ cations by doubly charged Ni^{2+} cations in the $LiSbF_6$ lattice results in half of the cation sites becoming vacant. The distribution of the Ni^{2+} sites and vacancies could be either ordered or disordered. If it is ordered, Ni^{2+} sites alternate with vacancies, and therefore the unit cell dimensions of $LiSbF_6$ must be doubled for $Ni(SbF_6)_2$.

A closer inspection of the powder pattern of $Ni(SbF_6)_2$ reveals indeed the presence of a weak line at 4.03Å. This line can only be indexed if the value of the c-axis of the hexagonal ($Z = 3$) $LiSbF_6$ unit cell is doubled, resulting in the following unit cell parameters for $Ni(SbF_6)_2$: $a = 5.16\text{Å}$, $c = 27.90\text{Å}$, $V = 643.3\text{Å}^3$, and $Z = 3$. Other super-structure lines were not observed, but their relative intensities might be very low. If the $Ni(SbF_6)_2$ pattern is indexed based on this doubled hexagonal cell, the rhombohedral condition, $-h + k + l = 3n$, obviously is no longer met.

On the other hand, if the distribution of the Ni^{2+} and vacancy sites were disordered, no super-structure lines should be observable. Consequently, the x-ray powder diffraction data of $Ni(SbF_6)_2$ are best interpreted in terms of a $LiSbF_6$ -type structure with an ordered occupation of the Li^+ sites by Ni^{2+} and vacancies.

In $LiSbF_6$ each Li is surrounded by six F from six different SbF_6^- octahedra [8]. Thus, both Li and Sb are hexacoordinated

TABLE I

X-RAY POWDER DATA FOR $\text{Ni}(\text{SbF}_6)_2^{\text{a}}$

d(obsd), Å	d(calcd), Å	Intens.	h	k	l
4.61	4.65	ms	0	0	6
4.24	4.26	s	1	0	2
4.03	4.03	w	1	0	3
3.75	3.76	s	0	1	4
2.744	2.750	ms	1	0	8
2.576	2.582	mw	1	1	0
2.363	2.367	m	0	1,10	
2.252	2.257	s	1	1	6
2.207	2.208	mw	0	2	2
2.125	2.129	mw	2	0	4
1.881	1.882	m	0	2	8
1.819	1.820	m	1	0,14	
1.745	1.745	w	2	0,10	
1.728	1.728	s	1	1,12	
1.681	1.678	m	2	1	2
1.646	1.643	m	1	2	4
1.625	1.625	w	0	1,16	
1.550	1.550	vw	0	0,18	
1.521	1.521	m	2	1	8
1.491	1.491	m	3	0	0
1.447	1.446	mw	1	2,10	
1.420	1.419	mw	3	0	6
1.377	1.375	w	2	0,16	
1.332	1.332	m	1	0,20	
1.292	1.291	mw	2	2	0
1.257	1.255	w	3	0	12
1.246	1.244	w	2	2	6
1.235	1.235	w	1	3	2
1.223	1.221	mw	1	3	4
1.216	1.214	mw	1	2	16

^aHexagonal; $a = 5.16\text{Å}$, $c = 27.90\text{Å}$, $Z = 3$, $V = 643.3\text{Å}^3$;
 CuK_α radiation, Ni filter.

with respect to fluorine, and each fluorine has one nearest Sb and Li neighbor. In $\text{Ni}(\text{SbF}_6)_2$ half of the Li sites of LiSbF_6 have been substituted with Ni while the other half is vacant. Assuming an ordered distribution of Ni sites and vacancies, only three of the six fluorines of each SbF_6^- anion can form fluorine bridges to Ni^{2+} cations. Furthermore, a close inspection of the LiSbF_6 structure suggests that for $\text{Ni}(\text{SbF}_6)_2$ the three bridging fluorines of each SbF_6^- anion must be cis with respect to each other, *i.e.* share a common face of the SbF_6 octahedron. Consequently, the site symmetry of the Sb atom in $\text{Ni}(\text{SbF}_6)_2$ may not be higher than C_{3v} .

A comparison of the unit cell of $\text{Ni}(\text{SbF}_6)_2$ with those of numerous other AMF_6 -type compounds [9] shows excellent agreement. The ionic radius of Ni^{2+} (0.69Å) [10] is similar to that of Li^+ (0.60Å) [9], and all the LiMF_6 -type compounds of [9] possess the rhombohedral-hexagonal LiSbF_6 structure. As discussed above, the $\text{Ni}(\text{SbF}_6)_2$ structure can be derived directly from the LiSbF_6 structure by converting the unimolecular rhombohedral LiSbF_6 cell to its corresponding trimolecular hexagonal cell, and then doubling the c-axis of the latter to accommodate a whole number of both, Ni^{2+} cation and vacancy sites.

A comparison of the powder pattern of $\text{Ni}(\text{SbF}_6)_2$ with that published for $\text{Ni}(\text{AsF}_6)_2$ [4] shows that the two compounds are not isotypic. This is unexpected because LiAsF_6 and NaAsF_6 are both isotypic with LiSbF_6 [9]. The pattern of $\text{Ni}(\text{AsF}_6)_2$ has previously been indexed [4] for a pseudo-cubic ($a/c = \sqrt{2}$), tetragonal unit cell with $a = 13.62$, $c = 9.63\text{Å}$, and $Z = 8$.

Vibrational Spectra

In A^+MF_6^- -type compounds, the nature and extent of the cation-anion interaction are of particular interest [4]. For $\text{B}^{2+}(\text{MF}_6^-)_2$ -type compounds, this interaction becomes even more interesting because only half of the fluorines can participate in bridges and the increased positive charge of the cations should result in stronger anion-cation attractions. As a consequence, the high symmetry of the MF_6^- anions in a compound such as LiSbF_6 [8] is

destroyed and vibrational spectroscopy should be well suited for the study of this problem.

According to the above x-ray data, the site symmetry of the SbF_6^- anions in $\text{Ni}(\text{SbF}_6)_2$ must be C_{3v} or lower and further splittings of bands are possible because the unit cell contains six SbF_6^- anions. The number of the possible fundamental vibrations and their expected infrared and Raman activities are shown in Table II for symmetry C_{3v} and the appropriate sub-groups. However, without knowledge of the space group and factor group of $\text{Ni}(\text{SbF}_6)_2$, a detailed analysis is not possible.

TABLE II

Correlation table for SbF_6^- IN $\text{Ni}(\text{SbF}_6)_2$

	free SbF_6^-	SbF ₆ ⁻ distorted by 3F bridges		
	O_h	C_{3v}	C_3	C_s
ν_{sym} in phase	A_{1g}	A_1	A	A'
ν_{sym} out of phase	E_g	E	E	A' A''
ν_{asym}	F_{1u}	A_1 E	A E	A' A' A''
δ_{sym}	F_{1u}	A_1 E	A E	A' A' A''
δ_{sym} in plane	F_{2g}	A_1 E	A E	A' A' A''
δ_{sym} out of plane	F_{2u}	A_1 E	A E	A' A' A''
IR active	F_{1u}	A_1, E	A, E	A', A''
RA active	A_{1g}, E_g, F_{2g}	A_1, E	A, E	A', A''

The observed infrared and Raman spectra are shown in Fig. 1 and the frequencies are summarized in Table III. In the frequency range expected for Sb-F stretching vibrations ($500\text{-}750\text{ cm}^{-1}$), at least eight infrared and seven Raman bands are observed which are not mutually exclusive. These data clearly indicate that SbF_6^- in $\text{Ni}(\text{SbF}_6)_2$ is not octahedral, but strongly distorted. The number of observed Sb-F stretching modes exceeds not only that (four) expected for either C_{3v} or C_3 symmetry, but also that (six) predicted for either C_s or C_1 symmetry, and is attributed to a low site symmetry of SbF_6^- and a dynamic coupling of the anions in the unit cell.

Based on frequency and intensity arguments, the following tentative assignments are proposed for the Sb-F stretching modes (see Table III). The three nonbridging fluorines should have higher frequencies and narrower and more intense Raman bands than the bridging ones. Furthermore, the symmetric stretching modes should be more intense in the Raman and the antisymmetric ones more intense in the infrared spectra. The relative sharpness of the nonbridging SbF_3 Raman bands lends additional support to our assumption of an ordered structure for $\text{Ni}(\text{SbF}_6)_2$.

For a disordered structure we would expect even more bands and, in particular, more diffuse Raman bands due to the irregularities in the fluorine bridging.

The bands in the $170\text{ to }320\text{ cm}^{-1}$ frequency range are assigned to the Sb-F deformation modes. As for the stretching modes, the frequency range covered by these vibrations is again considerably wider than, for example, for free SbF_6^- [11,12]. This effect is attributed to the influence of the fluorine bridges which will weaken the bridging Sb-F and strengthen the nonbridging Sb-F bonds. The frequency of a medium intensity infrared band with a very weak Raman counterpart in the 350 cm^{-1} region appears high for an Sb-F deformation mode, but is in the range expected for the Ni...FSb stretching mode and, therefore, is assigned accordingly.

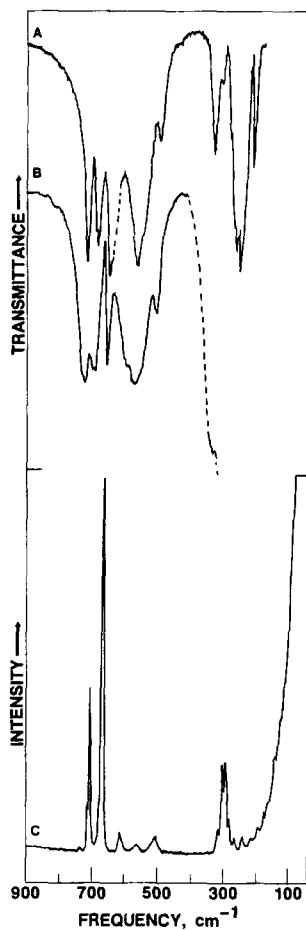


Fig. 1. Vibrational Spectra of Solid $\text{Ni}(\text{SbF}_6)_2$. Traces A and B, infrared spectra as KBr and AgCl pellets, respectively. The broken line in trace A probably contains a contribution from K SbF_6 generated by interaction of KBr with $\text{Ni}(\text{SbF}_6)_2$. The broken line in B is due to absorption by the AgCl window material. Trace C, Raman spectrum, recorded with a slit width of 5 cm^{-1} .

TABLE III

Vibrational frequencies and assignments for $\text{Ni}(\text{SbF}_6)_2$

Ir	obsd freq, cm^{-1} , and rel intens ^a	Ra	Assignment	
740vs	742(1)		vas SbF_3 out of phase	nonbridging SbF_3 stretching modes
716s	717(12)		vas SbF_3 in phase	
708s	710(44)		vsym SbF_3 out of phase	bridging SbF_3 stretching modes
673ms	674(100)		vsym SbF_3 in phase	
615sh	618(5)		vsym SbF_3 out of phase	bridging SbF_3 stretching modes
583s			vas SbF_3 out of phase	
568sh	568(2)		vas SbF_3 in phase	Ni...FSb stretching
521m	511(5)		vsym SbF_3 in phase	
354m	348(0+)			Sb-F deformations
331w	322(5)			
	308(24)			
302w	299(25)			
280s	287(9)			
267vs	272(3)			
	246(4)			
233m	220(1)			
	198(2)			
	172sh			
	146sh		Ni...F deformations	or lattice modes
	130sh			

^auncorrected Raman intensities based on relative peak heights

CONCLUSION

The above data demonstrate that, compared to $\text{Ni}(\text{AsF}_6)_2$ [3], $\text{Ni}(\text{SbF}_6)_2$ is thermally much more stable and is readily formed in high pressure-high temperature fluorination reactions involving SbF_5 in nickel reactors. X-ray powder diffraction data and vibrational spectra show that the $\text{Ni}(\text{SbF}_6)_2$ structure can be derived from the rhombohedral-hexagonal LiSbF_6 structure by substitution of the Li^+ cations by half as many Ni^{2+} cations and vacancies. The observation of a super-structure line in the x-ray powder data and the well defined and sharp Raman spectra support a structural model in which the Ni^{2+} sites and vacancies are ordered.

ACKNOWLEDGEMENT

The authors are grateful to Mrs. M. Lance, Mr. J. Isabey, Dr. C. J. Schack and Mr. R. D. Wilson for their help, to the US Army Research Office and the Office of Naval Research for financial support, and to Dr. R. Bau of the University of Southern California for the examination of $\text{Ni}(\text{SbF}_6)_2$ crystals by x-ray diffraction.

REFERENCES

- 1 J. P. Guertin, K. O. Christie, and A. E. Pavlath, *Inorg. Chem.*, 5 (1966) 1921.
- 2 W. E. Tolberg, R. T. Rewick, R. S. Stringham, and M. E. Hill, *Inorg. Chem.*, 6 (1967) 1156.
- 3 C. D. Desjardins and J. Passmore, *J. Fluorine Chem.*, 6 (1975) 379.
- 4 B. Frlec, D. Gantar, and J. H. Holloway, *J. Fluorine Chem.*, 19 (1982) 485.

- 5 P. A. W. Dean, *J. Fluorine Chem.*, 5 (1975) 499.
- 6 B. J. Hathaway and D. G. Holah, *J. Chem. Soc.*, (1964) 2400.
- 7 C. Hebecker, *Z. anorg. allgem. Chem.*, 376 (1970) 236.
- 8 J. H. Burns, *Acta Cryst.*, 15 (1962) 1098.
- 9 R. D. Kemmitt, D. R. Russell and D. W. A. Sharp, *J. Chem. Soc.*, (1963) 4408.
- 10 R. D. Shannon, *Acta Cryst. Part A*, 32 (1976) 751.
- 11 G. M. Begun and A. C. Rutenberg, *Inorg. Chem.*, 6 (1967) 2212.
- 12 K. O. Christe and C. J. Schack, *Inorg. Chem.*, 9 (1970) 2296.